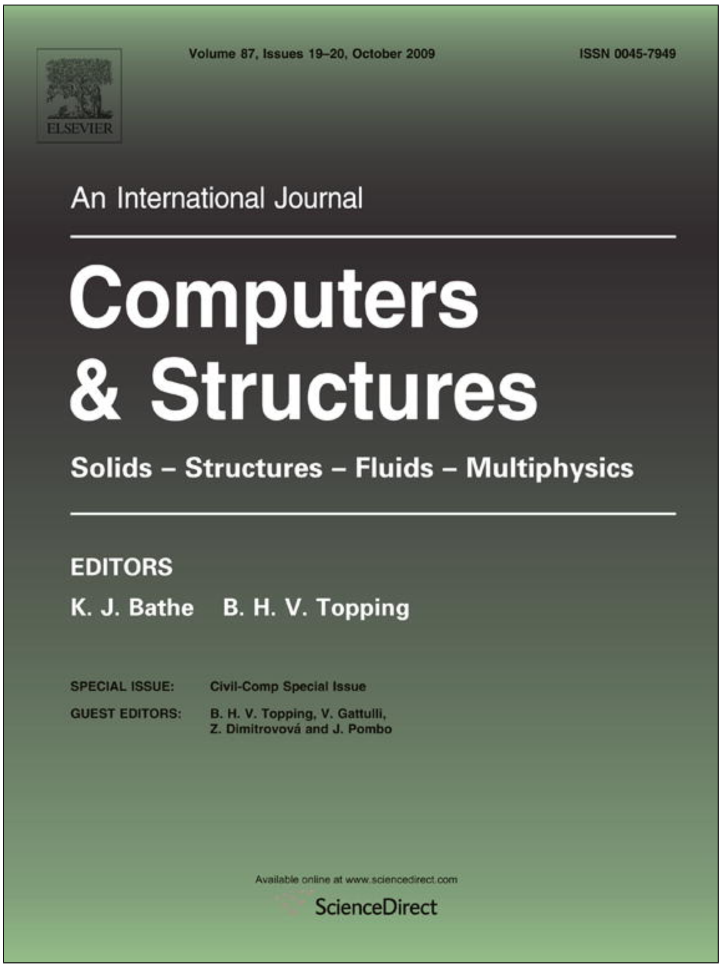
Volume 87, Issues 19–20, October 2009
ISSN 0045-7949
ELSEVIER
An International Journal
Computers & Structures
Solids – Structures – Fluids – Multiphysics
EDITORS
K. J. Bathe B. H. V. Topping
SPECIAL ISSUE: Civil-Comp Special Issue
GUEST EDITORS: B. H. V. Topping, V. Gattulli, Z. Dimitrovová and J. Pombo
Available online at www.sciencedirect.com
ScienceDirect

Computers and Structures 87 (2009) 1224–1232

Contents lists available at ScienceDirect

Computers and Structures

journal homepage: www.elsevier.com/locate/compstruc

Critical velocity of a load moving on a beam with a sudden change of foundation stiffness: Applications to high-speed trains

Z. Dimitrovová *, J.N. Varandas

UNIC, Department of Civil Engineering, New University of Lisbon, Monte da Caparica, Portugal

ARTICLE INFO

Article history:
Received 20 December 2007
Accepted 2 December 2008
Available online 12 January 2009

Keywords:
Foundation stiffness
Critical velocities
High-speed trains
Induced vibration
Moving load
Transition radiation

ABSTRACT

The transient dynamic response of a beam supported on a foundation with sudden stiffness change and subjected to a force moving with constant velocity is analysed. The abrupt change is located at the mid-section of the beam of finite length. Two analytical approaches are implemented. In the first one, the response is obtained by finite integral transformations incorporating global modes of vibration, while in the second the analytical responses of each half of the beam are linked by continuity conditions. The values obtained are used to study the influence of the abrupt change on the critical velocities. The analyses carried out enable to reach results and draw conclusions directly related to the knowledge of ground vibrations induced by high-speed trains.

1. Introduction

Mathematical representation of relatively complex physical phenomena plays a most important role in a vast number of technological problems that civil and mechanical engineering has to deal with, of which the development and improvement of transportation design is certainly one of the most challenging.

The constant growth of high-speed lines and the rapid evolution of train vehicles capable nowadays of reaching more than 500 km/h (138.9 m/s) gave raise to a number of specific related problems and have motivated a significant amount of scientific work. Some of the issues still demanding further attention can be listed: (i) attenuation of ground-borne vibrations on nearby residential areas; (ii) critical velocity analyses particularly pertinent when train lines have to cross soft soil areas or inhomogeneous regions; (iii) novel solutions guaranteeing low maintenance cost.

This paper deals with excessive ground and track vibrations induced by high-speed trains when moving from a region to another with a very different vertical stiffness of the system track-foundation. These vibrations, which have been observed and recorded, degrade rolling equipment and track and raise questions related to the vehicle stability and passengers comfort. Vertical stiffness change can be caused by sudden change of geotechnical foundations and/or structural solution, namely entering or leaving a viaduct or a bridge. The latter case covers also tunnels and transition from ballasted to concrete slab tracks and *vice versa*, where the vertical stiffness changes can be quite sharp. These scenarios have been already studied numerically and soil remedial solutions, attempting to gradually introduce the modifications of stiffness, are presented in [1].

First insight into a problem of induced vibrations can be acquired from simplified models that permit estimates of the response to a moving load travelling over a supporting structure. When the supporting structure changes, additional vibrations hereafter called transition radiation are generated. If the changes are abrupt, the amplitudes of these additional waves are significant and the dynamic response may be significantly more severe.

Transition radiation is studied in [2] for an elastic string and in [3] for several other systems including a beam subjected to a uniformly moving load, like the case presented below. The analytical solution shown in [3] is limited to a range of subcritical velocities and the effect of damping is not included. Other related analytical study [4] adds a moving mass to the model and assumes periodicity of the inhomogeneous characteristics of the foundation stiffness. A large number of numerical studies analyzing the additional vibration originated by track/foundation stiffness variation is also available, e.g. using the finite element method, [1], [5], stochastic analyses, [6], or experimental techniques [7].

In this paper analytical transient solutions of the dynamic response of one-dimensional finite systems with sudden change of foundation stiffness are presented. Two approaches are proposed, both without restrictions on load velocity and presence of damping. Results are expressed in terms of vertical displacement. The procedures are programmed in Matlab [8] and Maple [9]. Some of the results are confirmed using the general purpose finite element code ANSYS [10]. Nevertheless, it should be pointed out that, when using ANSYS, the authors detected that the higher natural

* Corresponding author.
E-mail address: zdim@fct.unl.pt (Z. Dimitrovová).

0045-7949/$ - see front matter © 2008 Civil-Comp Ltd. and Elsevier Ltd. All rights reserved.
doi:10.1016/j.compstruc.2008.12.005

frequencies were not accurately evaluated. This is confirmed in Cottrell et al. [11], who showed that such problem occurs for standard finite element formulations that make use of cubic Hermite polynomials as shape functions of the beam elements. This error, which for a given beam length depends on the ratio of the flexural rigidity to the mass per unit length of the beam, is inherent to the standard finite element method and cannot be solved by refining the mesh.

The procedures proposed in this paper consider exact values of the natural frequencies; thus, for simple cases, they are more accurate and faster than finite element analyses. Such procedures are used in a parametric study for determining the critical velocity. The study focuses on finite beams with arbitrary boundary conditions at the ends. However, real applications usually require extension to infinite situations. It is then necessary to eliminate the effect of the supports, mitigate the perturbation induced by the boundary conditions and prevent the reflection of travelling waves. This can be achieved without consideration of non-reflecting boundaries. In fact, it was verified, for realistic case studies in the subcritical velocity range, that the maximum displacement of the steady-state solution can be achieved within 100 m from the support. However, when the velocity is close to the critical value, this length must be extended.

In Section 2, the analytical form of the general transient dynamic solution for a beam subjected to a moving force [12] is extended to account for elastic foundation and damping, whereas in Section 3 the abovementioned two approaches are described. The first approach considers global modes of vibrations, which can be obtained by the displacement (sometimes called deformation) method extended to dynamics [13,14]. Having obtained the natural frequencies and modes, vertical displacements can be expressed analytically by generalized methods of integral transformations. A limiting factor is the laborious numerical calculation required for the determination of the natural frequencies, which can only be performed in codes such as Maple, due to the possibility of flexible numerical digits precision. Moreover, these frequencies are only valid for the particular structure under consideration. The main advantage of this approach, however, is that results can be evaluated only in places of interest, saving significant computational time. The second approach is based on the analytical expressions for the vertical displacement of two half-beams simply supported or clamped at one end and with non-homogeneous natural boundary conditions at the other (free) end. It is assumed that the Winkler constant is different in these two half-beams. Both solutions are made compatible and balanced through continuity conditions, that is, equality of vertical displacement and slope is prescribed in order to determine the unknown internal forces. The main advantage of this approach is that the natural frequencies of the two half-beams are known *a priori*. A disadvantage is that the internal forces must be determined numerically at each time step.

Both approaches permit to study the effects of the travelling force on chosen locations with different foundation stiffness in the full velocity range and presence of damping. As expected, simple supports are easier to deal with, especially in the first approach.

Section 4 contains the case studies definition and the interpretation of results. Section 5 is devoted to the critical velocities analysis and conclusions are given in Section 6.

It must be recognized that, in order to obtain a more realistic dynamic response, a vehicle spring–mass–damper system interacting with the rail must also be considered. This issue will be object of future developments.

2. Problem statement

In order to study transition radiation as the effect of sudden change of vertical stiffness of a railway track, transient analysis must be performed. With the purpose to obtain first insight into the problem, a simplified model composed of beam on elastic foundation is used. The study focuses on finite beams with either simple supports or clamped ends.

The governing displacement equation describing the dynamic response, under a constant moving load, P, of an Euler–Bernoulli's beam can be written as [12]:

$$EI\frac{\partial w^4(x,t)}{\partial x^4}+\mu\frac{\partial w^2(x,t)}{\partial t^2}+c\frac{\partial w(x,t)}{\partial t}=\delta(x-vt)P. \tag{1}$$

It is further assumed that the beam follows the linear elastic Hooke's law, has constant cross-section and constant mass per unit length, μ. As usually, small displacements, Navier's hypothesis and Saint-Venant's principle are adopted. E, I and c stand for Young's modulus, moment of inertia and coefficient of viscous damping, respectively; $w(x,t)$ represents the vertical deflection measured from the equilibrium position and oriented downwards, x is the spatial coordinate measured from left to right end of the beam, t is the time and $\delta(x)$ stands for the Dirac function of the abscissa x. It is assumed that the load moves with constant speed v. As usual in similar works, load inertia is omitted, although a methodology to account for the influence of the mass of the load is currently under development.

In order to include the effect of elastic foundation, characterized by Winkler's constant k, an additional term must be introduced into Eq. (1):

$$EI\frac{\partial w^4(x,t)}{\partial x^4}+\mu\frac{\partial w^2(x,t)}{\partial t^2}+c\frac{\partial w(x,t)}{\partial t}+kw(x,t)=\delta(x-vt)P. \tag{2}$$

The boundary conditions will be given further and the initial conditions (given below) are homogeneous:

$$w(x,0)=0,\quad \left.\frac{\partial w(x,t)}{\partial t}\right|_{t=0}=0. \tag{3}$$

If, as in [12,13], the circular frequency of damping ω_b is introduced, the coefficient of damping c can be replaced in Eqs. (1) and (2) by the term $2\mu\omega_b$. The difference is the following: the coefficient of damping can be interpreted as the damping of the foundation modelled by distributed dashpots. The circular frequency of damping can account for mass damping in the beam, i.e. $2\omega_b$ expresses the mass damping coefficient. The circular frequency of damping simplifies some of the expressions given below (Eqs. (8) and (9)) and has the advantage that is connected with the concept of critical damping, because then the viscous damping factor ξ corresponds to the ratio $\omega_b/\omega_{(j)}$. However, the circular frequency of damping actually varies with the natural frequency, therefore the symbol ω_{bj}, usually linked to the logarithmic decrement ϑ by $\omega_{bj}=\vartheta f_{(j)}$ (where $f_{(j)}$ is the jth natural frequency), will be used from now on.

The solution of Eq. (2) is assumed as an expansion in series:

$$w(x,t)=\sum_{j=1}^{\infty}W(j,t)\frac{w_{(j)}(x)}{W_j}, \tag{4}$$

where the transform $W(j,t)$ of the original $w(x,t)$ reads as:

$$W(j,t)=\int_0^L w(x,t)w_{(j)}(x)dx, \tag{5}$$

$w_{(j)}$ stands for the jth beam natural undamped vibration mode:

$$w_{(j)}(x)=A_j\sin\frac{\lambda_j x}{L}+B_j\cos\frac{\lambda_j x}{L}+C_j\sinh\frac{\lambda_j x}{L}+D_j\cosh\frac{\lambda_j x}{L} \tag{6}$$

and

$$W_j=\int_0^L \mu w_{(j)}^2(x)dx. \tag{7}$$

By use of the Laplace–Carson transformation applied to the governing equation (2) expressed in terms of $W(j,t)$, it yields:

$$W(j,t) = \frac{1}{b_{(j)}} \int_0^t P w_{(j)}(v\tau) e^{-a(t-\tau)} \sin(b_{(j)}(t-\tau)) d\tau, \tag{8}$$

where

$$a = \omega_{bj}, \quad b_{(j)} = \sqrt{\omega_{(j)}^2 - \omega_{bj}^2}. \tag{9}$$

$\omega_{(j)}$ stands for the jth natural frequency of the beam and $b_{(j)}$ represents the frequency of the damped free vibration.

In regions with a constant Winkler foundation, $\omega_{(j)}$ can be expressed as:

$$\omega_{(j)} = \sqrt{\frac{\lambda_j^4}{L^4}\frac{EI}{\mu} + \frac{k}{\mu}}. \tag{10}$$

If the Winkler foundation is constant along the beam, λ_j is uniquely defined by the corresponding characteristic equation, and λ_j/L is usually designated as the flexural wave number of the beam. For simple supports:

$$\lambda_j = j\pi; \quad A_j = 1; \quad B_j = C_j = D_j = 0 \ \forall j. \tag{11}$$

For clamped ends λ_j corresponds to the roots of the following equation:

$$\cos\lambda_j \cosh\lambda_j - 1 = 0, \tag{12}$$

B_j is calculated as:

$$B_j = -\frac{\sin\lambda_j - \sinh\lambda_j}{\cos\lambda_j - \cosh\lambda_j} \tag{13}$$

and $A_j = 1$, $C_j = -1$ and $D_j = -B_j$, $\forall j$.If a cantilever beam is assumed, irrespectively of the beam being clamped on the right or on the left hand side, λ_j corresponds to the roots of:

$$1 + \cos\lambda_j \cosh\lambda_j = 0, \tag{14}$$

B_j is calculated by:

$$B_j = -\frac{\sin\lambda_j + \sinh\lambda_j}{\cos\lambda_j + \cosh\lambda_j} \tag{15}$$

for right clamping $A_j = C_j = 1$, $D_j = B_j \ \forall j$ and for left clamping $A_j = 1$, $C_j = -1$ $D_j = -B_j \ \forall j$.

3. The case of sudden change of vertical stiffness

It is assumed that there is an abrupt change of the Winkler constant at mid span of the beam, k_1 and k_2 designating its value on each region of length L.

3.1. Superposition of global modes

The global modes of vibration can be obtained from the solution of the equations formulated by the displacement method for frame structures extended to dynamics [13,14]. Eq. (6) is applied to each region, with distinct arguments λ_1 and λ_2 and distinct constants affecting the trigonometric and hyperbolic functions. As the natural frequency must be unique for each mode:

$$\omega_{(j)} = \sqrt{\frac{\lambda_{1,j}^4}{L^4}\frac{EI}{\mu} + \frac{k_1}{\mu}} = \sqrt{\frac{\lambda_{2,j}^4}{L^4}\frac{EI}{\mu} + \frac{k_2}{\mu}}, \tag{16}$$

permitting to express λ_1 as a function of λ_2 or *vice versa*. In a standard way, λ_1 or λ_2 can be seen as roots of the determinant of the global dynamic stiffness matrix composed by the coefficients of the equilibrium conditions in terms of the unknown displacement and rotation at the middle beam section [13]. The expression of the determinant is rather simple, because only two global degrees of freedom are involved. Alternatively, the determinant of the coefficients of the four continuity conditions could be used. The analytical solution is expressed by Eqs. (4), (7), and (8) can be used in the same form as before, but over the full beam length $2L$.

However, Eq. (16) is not simple to implement into the determinant and the roots are quite difficult to find. Generally, if $k_2 > k_1$, the first global modes of vibration affect only the softly supported part of the beam. These modes are distinguished by the fact that λ_1 is a small real positive number, yielding negative λ_2^4. This is only possible if λ_2 is a complex number, in which the real and the imaginary part are the same in absolute values. Consequently, some of the constants from Eq. (6) are also complex numbers, although not implying imaginary components in the displacement field. In such cases, finding the roots becomes numerically very sensitive. For instance, assuming $k_1 = 427\ \mathrm{kN/m^2}$ per unit beam length, $k_2/k_1 = 8$ and other beam characteristics as described in Section 3, displacements in the soft part are dominant for the 22 first modes. In this case, it was sometimes necessary to use a 60 digits precision to find the corresponding roots. In addition to numerical difficulties, the modes of vibration obtained this way are only valid for the particular structure under consideration. Nevertheless, the main advantage of such approach is that, results can be directly evaluated only in places of interest.

The procedure for finding the roots was programmed in Maple, where the numerical precision is easy adjustable. More difficulties were encountered for clamped ends, because of the more complex expression of the determinant of the global dynamic stiffness matrix. The number of modes needed for accurate results depends on the total beam length and on the expected minimum wave length in the analysis. It was verified that high number of modes must be used in examples presented in this paper in order to approximate well the transient displacement field. The reason is that the quasi-steady-state deflection shape must be formed in the first part of the structure, and then this shape is perturbed by radiation waves. 350 modes were used to obtain the results presented in this paper. It was confirmed by convergence study that 200 modes would have been sufficient for most cases, in which the total beam length was assumed as 200 m. Then dominating displacement values around the discontinuity in the elastic foundation were approximated with 3% precision with respect to the numerical results from ANSYS. However, 350 modes were necessary to implement in the analysis in order to reach the same precision in the deflections of the beam with the total length of 800 m.

3.2. Joint solution of two half-beams

In order to avoid the difficulties in finding roots described in the previous section, an alternative procedure is proposed. In this procedure, the dynamic responses of two half-beams are solved separately and joined together by continuity equations. The point of Winkler constant discontinuity corresponds to the point of beam continuity, therefore equilibrium of internal forces must be preserved and equality of vertical displacement and of its spatial derivative (slope) must be maintained at that point. The solution of the continuity equations is not straightforward and must be done numerically.

It was verified that a half-beam with simple support on one side could be considered, because both kinds of boundary conditions, essential and natural, are used to determine the natural modes of vibrations according to Eq. (6). Nevertheless, since this half-beam is geometrically indeterminate, a mode of vibration corresponding to a rigid body motion (rotation around the support), must also be taken into account. In such case, $\omega_{(0)} = \sqrt{k_1/\mu}$ for the left half and analogously $\omega_{(0)} = \sqrt{k_2/\mu}$ for the right half. Further modes have as argument λ_j, corresponding to roots of:

$$\cos\lambda_j \sinh\lambda_j - \sin\lambda_j \cosh\lambda_j = 0, \tag{17}$$

C_j is calculated as:

$$C_j = \frac{\sin\lambda_j}{\sinh\lambda_j} \tag{18}$$

$A_j = 1$ and $B_j = D_j = 0$, $\forall j$ .Finding the roots of Eqs. (14) and (17) is simple. In addition, after the 10 or 20 first roots, depending of the precision required, further values can be estimated by $\lambda_{j+1} = \lambda_j + \pi$ for Eq. (14) and by $\lambda_j = j\pi + \pi/4$ for Eq. (17). Moreover, for each kind of boundary conditions, λ-values are uniquely defined independently of other beam input data and assumed value for Winkler constant.

Then, the two "half" solutions, corresponding to beams supported on left and right hand side, with different values of Winkler constant, are connected together by compatibility conditions.

First of all, the dynamic response must be expressed for non-homogeneous natural boundary conditions at the free end. Hence, the transform, $W(j,t)$, given previously by Eq. (8), must be modified to:

$$W(j,t) = \frac{1}{b_{(j)}} \int_0^t (Pw_{(j)}(\upsilon\tau) - EIz(0,L,\tau))e^{-a(t-\tau)} \sin(b_{(j)}(t-\tau))d\tau. \tag{19}$$

where

$$\begin{aligned} z(0,L,t) &= -\frac{V(L,t)}{EI} w_{(j)}(L) + \frac{M(L,t)}{EI} \left.\frac{dw_{(j)}(x)}{dx}\right|_{x=L}, \\ z(0,L,t) &= \frac{V(0,t)}{EI} w_{(j)}(0) - \frac{M(0,t)}{EI} \left.\frac{dw_{(j)}(x)}{dx}\right|_{x=0} \end{aligned} \tag{20}$$

for the left and right supports, respectively. V and M stand for transverse force and bending moment with usual conventions from Mechanics of Materials. Since it was assumed that both half-beams have the same length L, it is convenient to introduce a spatial variable measured from the supported ends. This way, Eq. (19) has the same form for the left and the right half of the full beam and the only difference is in $b_{(j)}$, given by Eqs. (9) and (10). Thus:

$$\begin{aligned} W^{\mathrm{L}}(j,t) = \frac{1}{b^{\mathrm{L}}_{(j)}} \Bigg\{ &\int_0^t Pw_{(j)}(\upsilon\tau)e^{-a(t-\tau)} \sin(b^{\mathrm{L}}_{(j)}(t-\tau))d\tau \\ &+ \int_0^t \left(V(L,\tau)w_{(j)}(L) - M(L,\tau)\left.\frac{dw_{(j)}(x)}{dx}\right|_{x=L} \right) e^{-a(t-\tau)} \\ &\times \sin(b^{\mathrm{L}}_{(j)}(t-\tau))d\tau \Bigg\} = \end{aligned} \tag{21}$$

$$\begin{aligned} W^{\mathrm{R}}(j,t) = \frac{1}{b^{\mathrm{R}}_{(j)}} \Bigg\{ &\int_0^t Pw_{(j)}(\upsilon\tau)e^{-a(t-\tau)} \sin(b^{\mathrm{R}}_{(j)}(t-\tau))d\tau \\ &+ \int_0^t \left(V(L,\tau)w_{(j)}(L) + M(L,\tau)\left.\frac{dw_{(j)}(x)}{dx}\right|_{x=L} \right) e^{-a(t-\tau)} \\ &\times \sin(b^{\mathrm{R}}_{(j)}(t-\tau))d\tau \Bigg\} = \end{aligned} \tag{22}$$

where the superscripts L and R stand for the left and the right hand side of the full beam, respectively. The main difficulty lies in the fact that the internal forces must be integrated over time when their actual values and their time variation are unknown. Therefore, assumption about time variation of internal forces at the section of discontinuity must be adopted and the time interval must be discretized.

Assuming piece-wise constant distribution of the internal forces at the elastic stiffness change, it can be written for the left part:

$$\begin{aligned} W^{\mathrm{L}}(j,t) &= \frac{1}{b^{\mathrm{L}}_{(j)}} \int_0^t Pw_{(j)}(\upsilon\tau)e^{-a(t-\tau)} \sin(b^{\mathrm{L}}_{(j)}(t-\tau))d\tau \\ &\quad + \frac{1}{b^{\mathrm{L}}_{(j)}} \sum_{s=0}^{k} \left(V(s)w_{(j)}(L) - M(s)\left.\frac{dw_{(j)}(x)}{dx}\right|_{x=L} \right) \\ &\quad \times \int_{t_s}^{t_{s+1}} e^{-a(t-\tau)} \sin(b^{\mathrm{L}}_{(j)}(t-\tau))d\tau \\ &= \frac{1}{b^{\mathrm{L}}_{(j)}} \int_0^t Pw_{(j)}(\upsilon\tau)e^{-a(t-\tau)} \sin(b^{\mathrm{L}}_{(j)}(t-\tau))d\tau \\ &\quad + \frac{1}{b^{\mathrm{L}}_{(j)}} w_{(j)}(L) \sum_{s=0}^{k} V(s) \int_{t_s}^{t_{s+1}} e^{-a(t-\tau)} \sin(b^{\mathrm{L}}_{(j)}(t-\tau))d\tau \\ &\quad - \frac{1}{b^{\mathrm{L}}_{(j)}} \left.\frac{dw_{(j)}(x)}{dx}\right|_{x=L} \sum_{s=0}^{k} M(s) \int_{t_s}^{t_{s+1}} e^{-a(t-\tau)} \sin(b^{\mathrm{L}}_{(j)}(t-\tau))d\tau \\ &= \tilde{P}^{\mathrm{L}}(j,k) + \tilde{V}^{\mathrm{L}}(j,k-1) + \frac{V(k)}{b^{\mathrm{L}}_{(j)}} w_{(j)}(L) \\ &\quad \times \int_{t_k}^{t_{k+1}} e^{-a(t-\tau)} \sin(b^{\mathrm{L}}_{(j)}(t-\tau))d\tau - \tilde{M}^{\mathrm{L}}(j,k-1) \\ &\quad - \frac{M(k)}{b^{\mathrm{L}}_{(j)}} \left.\frac{dw_{(j)}(x)}{dx}\right|_{x=L} \int_{t_k}^{t_{k+1}} e^{-a(t-\tau)} \sin(b^{\mathrm{L}}_{(j)}(t-\tau))d\tau. \end{aligned} \tag{23}$$

Using an analogous expression for the right hand side one obtains:

$$\begin{aligned} W(j,t) &= \tilde{P}^{\mathrm{R}}(j,k) + \tilde{V}^{\mathrm{R}}(j,k-1) + \frac{V(k)}{b^{\mathrm{R}}_{(j)}} w_{(j)}(L) \int_{t_k}^{t_{k+1}} e^{-a(t-\tau)} \\ &\quad \times \sin(b^{\mathrm{R}}_{(j)}(t-\tau))d\tau + \tilde{M}^{\mathrm{R}}(j,k-1) \\ &\quad + \frac{M(k)}{b^{\mathrm{R}}_{(j)}} \left.\frac{dw_{(j)}(x)}{dx}\right|_{x=L} \int_{t_k}^{t_{k+1}} e^{-a(t-\tau)} \sin(b^{\mathrm{R}}_{(j)}(t-\tau))d\tau. \end{aligned} \tag{24}$$

In Eqs. (23), (24), $V(s)$ and $M(s)$ stand for the values of the internal forces at the discontinuity in the time interval $t \in (t_s, t_{s+1}]$, with $t_0 = 0$.

At a new time step $t = t_{k+1}$, the values for $s = 0, \ldots, k$ are known, because they were computed in previous time steps and the only unknowns $V(k)$ and $M(k)$ can be determined from continuity of displacement and slope at the place of the stiffness change. It is more convenient to perform this calculation numerically. Nevertheless, expressing the solution of these two equations analytically, a full solution would be possible to obtain by recursive analytical form.

The procedure is programmed in Matlab. For the sake of simplicity, it is assumed that the time interval is divided uniformly in small steps (since obviously an accurate solution requires a fine time discretization). As Matlab does not allow increasing of numerical precision, a full calculation was possible only with 200 vibration modes involved. This represents a limitation of the procedure. Convergence studies were performed as in the previously described approach. It was again confirmed that 200 modes are sufficient in cases, in which the total beam length is assumed as 200 m. However, in the analysis of the beam with the total length of 800 m implementation of only 200 modes yield approximately 30% error in dominating displacements around the discontinuity in foundation, with respect to the numerical results from ANSYS. Because of this limitation, the procedure described in this section was also programmed in Maple, in order to take advantage of the flexible numerical digits precision, required in higher frequencies modes.

4. Validation and analysis of results

In order to validate the procedures proposed above, an equivalent model was created using ANSYS [10]. Element BEAM 54 of the ANSYS library, with the capacity of introduction of elastic foundation, was used. Since ANSYS does not allow direct moving load implementation, for each time step a new force position had to be considered, according to the load speed and the element size. Having in mind possible errors depicted in [11], it was decided to analyse a simply supported beam with 100 m length and a coefficient of the elastic foundation stiffness ranging from 0.5 to 100 MN/m^2 (typical values for practical applications). For full track beam models (high ratio of the flexural rigidity to the mass per unit length), independently of the foundation stiffness, the error in the natural frequencies of the flexural modes obtained by ANSYS with respect to the analytical values was 25.9% in the 100th mode and 78.5% in the 500th mode. Moreover, for a foundation stiffness of 10 MN/m^2, the first three modes were interchanged, in the way that the expected first mode shape appeared in the third position. For a foundation stiffness of 100 MN/m^2 the first 11 mode shapes were interchanged among themselves. However, when two standard European rails UIC60 were modelled (low ratio of the flexural rigidity to the mass per unit length) the error in the natural frequencies became much lower, i.e. 1.9% in the 100th mode and 29.0% in the 500th mode. In this case, for a foundation stiffness of 100 MN/m^2, only the first five mode shapes were interchanged. For these reasons, verification analyses were performed only in cases where the beam is modelled as two standard European rails UIC60 supported by relatively soft foundation.

Damping was modelled in two ways; first, the element damping parameter c of distributed dashpots was used, and then the mass coefficient $\alpha = 2\omega_b$ of Rayleigh damping was implemented. In both cases, only constant values without dependence on natural frequencies were used. With the purpose to test the analytical formulas from Section 2, several tests were run; covering sub- and supercritical damping cases as well as sub- and supercritical velocity cases. It was found that the computed displacement field matched exactly the analytical solution, confirming the suitability of the strategy adopted for the analysis and suggesting that it is possible to solve numerically other situations impossible to treat analytically, but with the limitations previously outlined.

In order to show the generation of radiation waves, two scenarios are examined herein. Damping is not considered in these analyses in order to better visualize the induced vibrations.

The first example (Case study 1) uses input parameters similar as in [3] and the second one is related to rather strong foundation conditions (Case study 2). In both cases, the beam models two standard rails UIC60 and the elastic foundation includes the properties of the full railway system and soil. The applied load was approximated by a total axle mass of 17000 kg corresponding to a locomotive of the Thalys high-speed train. All numerical input data are summarized in Table 1.

Very weak foundation conditions are implemented as in [3], namely $k_1 = 427$ kN/m^2 is used in the soft region and $k_2 = 854$ kN/m^2 in the strong one. According to [12], the critical velocities corresponding to steady-state situations with homogeneous foundation $k = 427$ kN/m^2 and $k = 854$ kN/m^2 are: 197.6 m/s and 235.0 m/s, respectively. Parts with different foundation have 400 m length and the origin of the spatial coordinate system is connected to the section of discontinuity. As in [3], a velocity $v = 188.65$ m/s was chosen, which is very close to the critical velocity of the soft region. Attention is paid to transition radiation. It is known, that in the steady-state situation with homogeneous foundation, when the load velocity approaches the critical value, the ratio between the upward and the downward maximum displacement is large (around 0.5). Therefore, if there is an abrupt change in the vertical stiffness, the radiation waves will have large amplitude. This will be seen in the following figures.

Load positions corresponding to 1 m before discontinuity, 7 m, 60 m and 90 m after discontinuity were chosen as representative. It is seen in all cases that the solution obtained by Maple following the procedure highlighted in Section 3.1 is in excellent agreement with the results presented in [3]. Deflection curves are summarized in Figs. 1–4. Figs. 1 and 2 illustrate the high increase in downward and upward displacement right before and right after the discontinuity, respectively. Figs. 3 and 4 show the development and separation of the transition wave.

Further verification was performed for the same situation as described above but with double velocity (377.3 m/s). Such velocity is above the critical velocities for both parts and is impossible to be reached by any high-speed train. In this case, the solution from [3] is not valid any more and therefore the comparison is done

Table 1
Numerical input data used in case studies

Property	Beam (2 rails UIC60)
Young's modulus (GPa)	210
Moment of inertia (m^4)	6110×10^{-8}
Density per unit length (kg/m)	119.87
	Foundation
Winkler constant per unit length in soft region – case study 1 (kN/m^2)	427
Winkler constant per unit length in strong region – case study 1, test value 1 (kN/m^2)	854
Winkler constant per unit length in strong region – case study 1, test value 2 (kN/m^2)	1708
Winkler constant per unit length in strong region – case study 1, test value 3 (kN/m^2)	3416
Winkler constant per unit length in soft region – case study 2 (kN/m^2)	20000
Winkler constant per unit length in strong region – case study 2 (kN/m^2)	40000
	Load
Test load (kN)	166.8

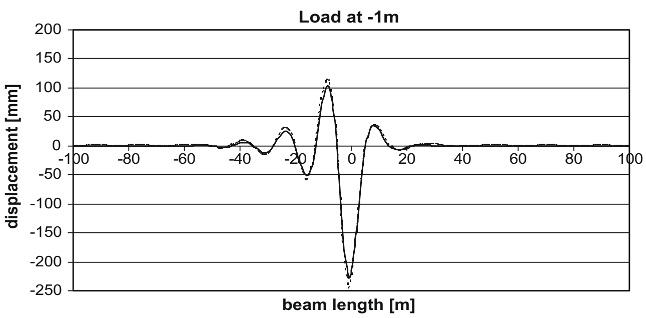

Fig. 1. Deflection curves for load position at −1 m. Solution from [3] (full line) and solution according to Section 3.1 (dashed line), $v = 188.65$ m/s.

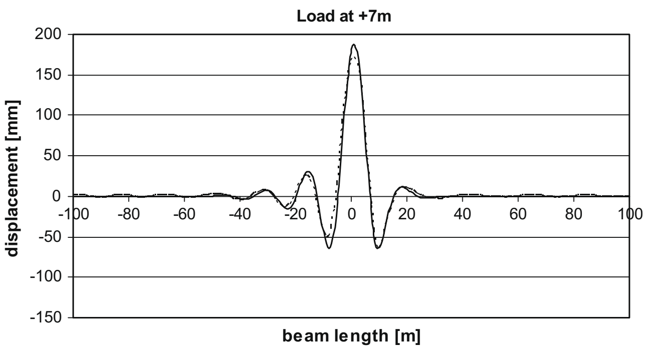

Fig. 2. Deflection curves for load position at +7 m. Solution from [3] (full line) and solution according to Section 3.1 (dashed line), $v = 188.65$ m/s.

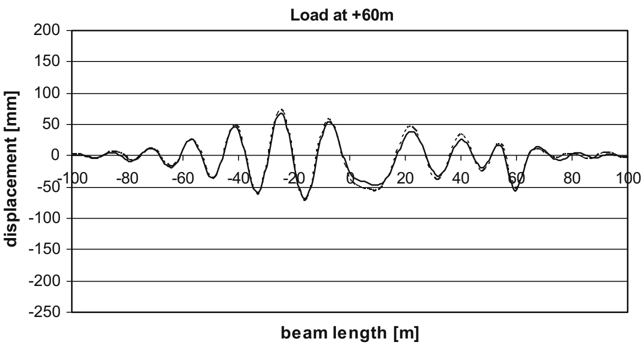

Fig. 3. Deflection curves for load position at +60 m. Solution from [3] (full line) and solution according to Section 3.1 (dashed line), v = 188.65 m/s.

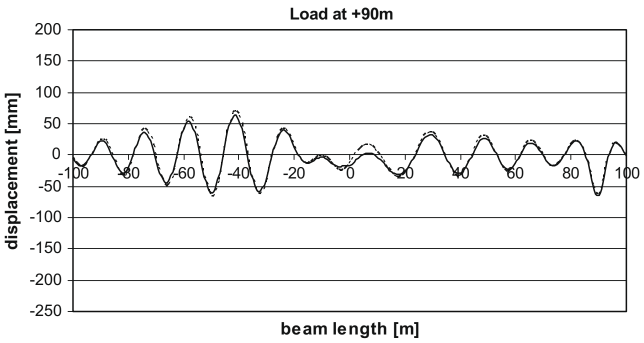

Fig. 4. Deflection curves for load position at +90 m. Solution from [3] (full line) and solution according to Section 3.1 (dashed line), v = 188.65 m/s.

against ANSYS software. Only force positions −1 and +60 m were chosen. The results are summarized in Figs. 5 and 6. From this comparison, it can be proven that the proposed methodology is valid irrespectively of the velocity of the moving load.

The case study 2 aims to reproduce the situation of a high-speed train on rather strong foundation conditions. Reference values of 20 MN/m^2 and 40 MN/m^2 per unit beam length were chosen in the soft and in the strong regions of equal length 100 m, respectively. The critical velocity corresponding to the steady-state situation with a homogeneous foundation of 20 MN/m^2 is 517 m/s. It was assumed that the train travels at a velocity of 200m/s, which is greater than the maximum operating high-speed train velocity ever recorded. It can be seen that, for this velocity, the radiation waves are hardly noticeable.

The results are given in Figs. 7–11. First of all, it is shown that downward maximum displacement of the corresponding steady-state solution is reached in both regions and the effect of end supports is small, but visible, as expected in the transient solution. This is visualized in Fig. 7, where the response is plotted for load position at −40, −1, +8 and +60 m, respectively. In order to show small radiation waves, the same case in augmented scale is given in Fig. 8.

Next, still in subcritical velocity range, but for a much higher value v = 500 m/s, which has now only academic meaning, transition radiation is clearly visualized, but also the effect of supports and reflecting waves is more significant. It is seen again that just before the discontinuity there is a sudden increase in downward displacements (Fig. 9) and right after the discontinuity there is a sudden increase in upward displacement (Fig. 10).

After the load passes the section of discontinuity in foundation, transition radiation waves are generated in form of additional

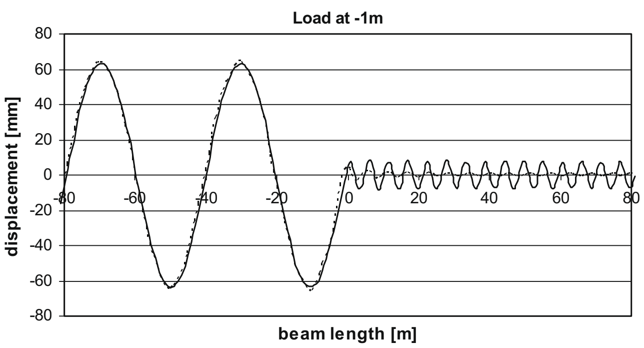

Fig. 5. Deflection curves for load position at −1 m. Solution by ANSYS (full line) and solution according to Section 3.1 (dashed line), v = 377.3 m/s.

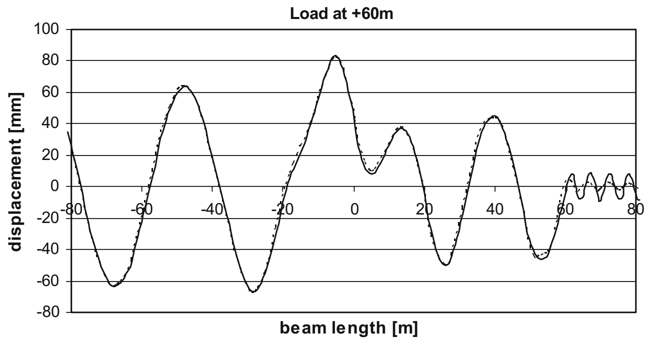

Fig. 6. Deflection curves for load position at +60 m. Solution by ANSYS (full line) and solution according to Section 3.1 (dashed line), v = 377.3 m/s.

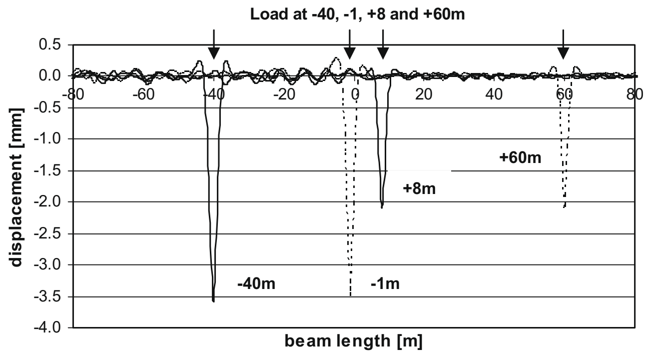

Fig. 7. Deflection curves for load position at −40, −1, +8 and +60 m, respectively (v = 200 m/s).

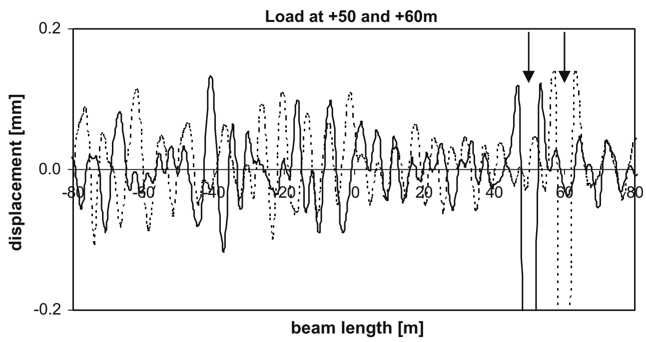

Fig. 8. Deflection curves for load position at +50 m (full curve) and +60 m (dashed curve) (v = 200 m/s), showing transition radiation.

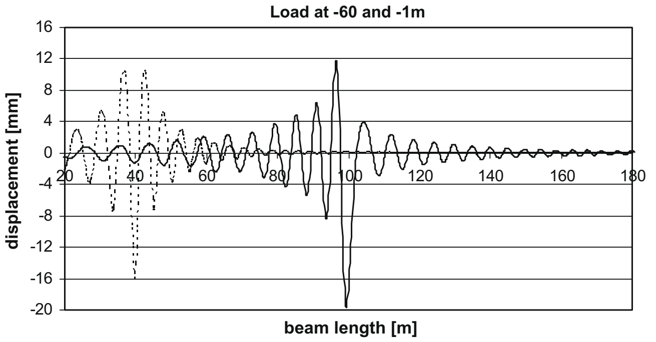

Fig. 9. Deflection curves for load position at −60m (dashed curve) and −1 m (full curve), respectively, (v = 500 m/s).

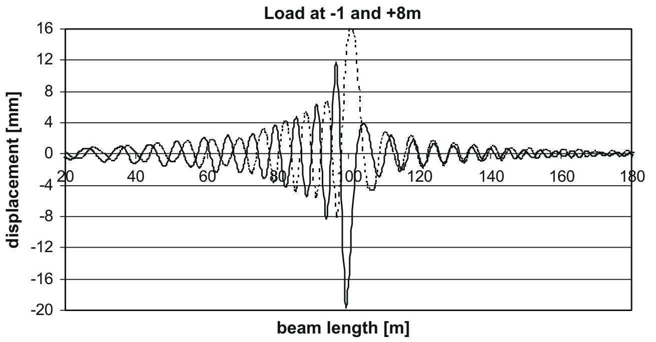

Fig. 10. Deflection curves for load position at −1 m (full curve) and +8 m (dashed curve), respectively, (v = 500 m/s).

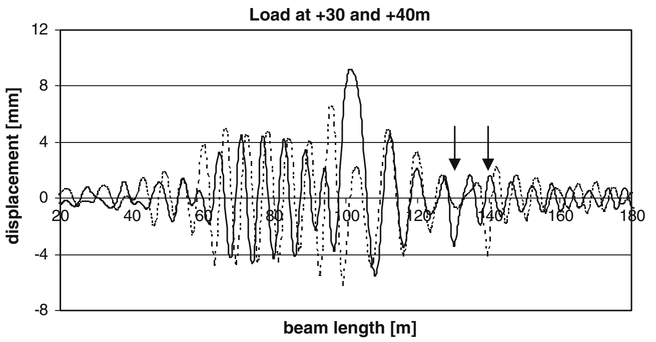

Fig. 11. Deflection curves for load position at +30 m (full curve) and +40 m (dashed curve), respectively, (v = 500 m/s).

waves emerging from this section and travelling in both directions, but mainly visible in the soft part of the structure (Fig. 11).

In some of the figures above, the displacements are quite high and therefore the assumption of small deflection theory may be questionable. Nevertheless, it is most likely that in the non-linear range these figures would be qualitatively similar and would continue to highlight the potential danger of displacement increase due to the sudden change in foundation stiffness.

Displacements in all figures are plotted with negative sign, in order to preserve their orientation upward or downward.

5. Critical velocities by parametric analysis

Global critical velocities are examined by parametric analysis. The procedure is programmed in Maple and it exploits the methodology described in Section 3.2. Input data correspond to the Case study 1, as specified in Table 1, namely k_1 = 427 kN/m^2 is implemented in the soft region and then three cases with k_2/k_1 = 2, 4 and 8 are considered. In these three situations the load is supposed either to move from the soft to strong part or *vice versa*, giving in total six test cases. The critical velocities corresponding to the load moving on the same beam, but with homogeneous foundation of k = 427 kN/m^2, k = 854 kN/m^2, k = 1708 kN/m^2 and k = 3416 kN/m^2, are: 197.6m/s; 235.0 m/s; 279.5 m/s and 332.4 m/s, respectively.

Results are summarized in Figs. 12–17. In Figs. 12–14 passage from the soft to the strong part with three assumed rations of Win-

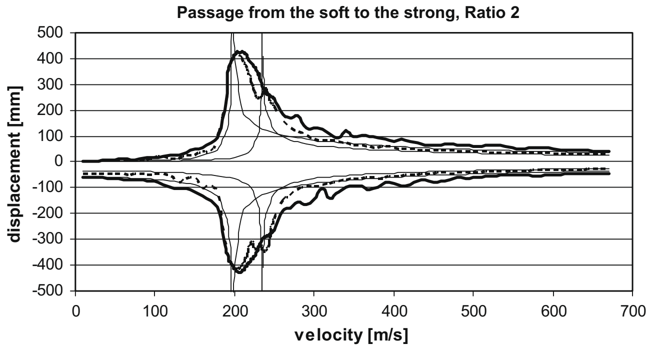

Fig. 12. Maximum downward and upward displacements with respect to velocity for force passage from the soft to the strong region of ratio 2, maxima in the soft part (full thick curves), maxima in the strong part (dashed thick curves) and maxima from steady-state solutions on homogeneous foundation (thin curves).

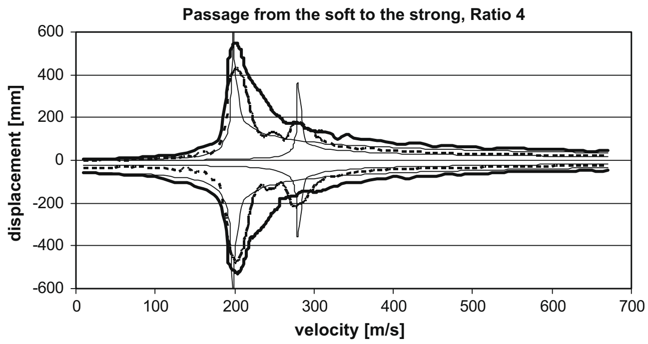

Fig. 13. Maximum downward and upward displacements with respect to velocity for force passage from the soft to the strong region of ratio 4, maxima in the soft part (full thick curves), maxima in the strong part (dashed thick curves) and maxima from steady-state solutions on homogeneous foundation (thin curves).

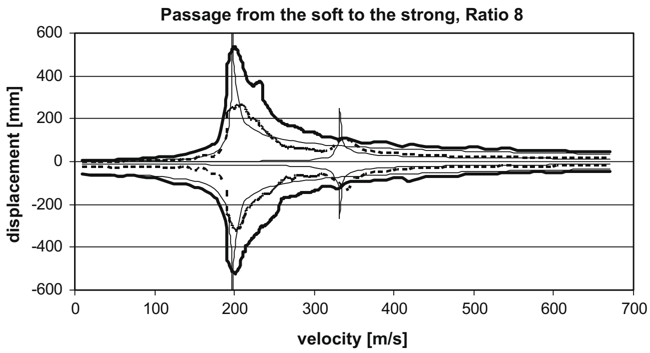

Fig. 14. Maximum downward and upward displacements with respect to velocity for force passage from the soft to the strong region of ratio 8, maxima in the soft part (full thick curves), maxima in the strong part (dashed thick curves) and maxima from steady-state solutions on homogeneous foundation (thin curves).

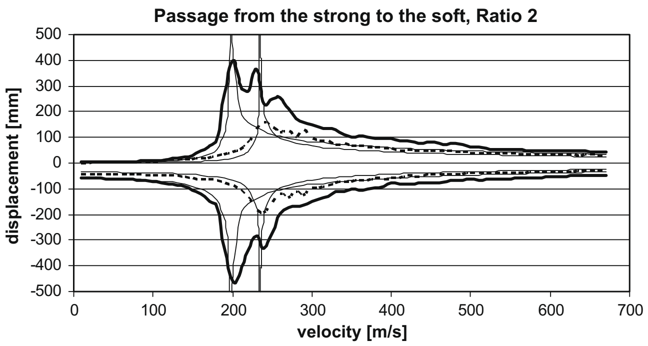

Fig. 15. Maximum downward and upward displacements with respect to velocity for force passage from the strong to the soft region of ratio 2, maxima in the soft part (full thick curves), maxima in the strong part (dashed thick curves) and maxima from steady-state solutions on homogeneous foundation (thin curves).

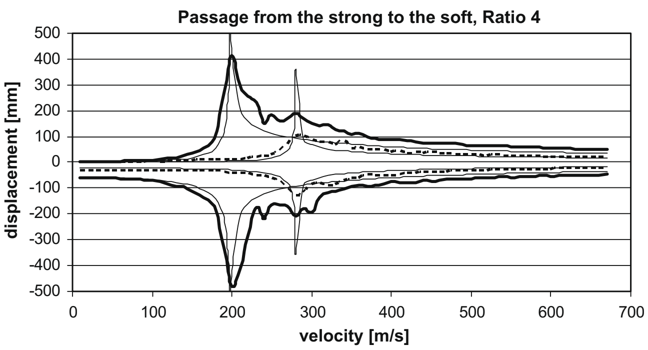

Fig. 16. Maximum downward and upward displacements with respect to velocity for force passage from the strong to the soft region of ratio 4, maxima in the soft part (full thick curves), maxima in the strong part (dashed thick curves) and maxima from steady-state solutions on homogeneous foundation (thin curves).

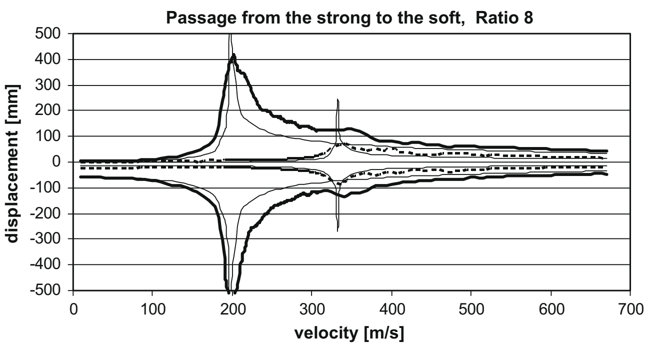

Fig. 17. Maximum downward and upward displacements with respect to velocity for force passage from the strong to the soft region of ratio 8, maxima in the soft part (full thick curves), maxima in the strong part (dashed thick curves) and maxima from steady-state solutions on homogeneous foundation (thin curves).

kler constant 2, 4 and 8 are considered. Maximum displacement directed downward as well as upward is plotted separately for the first and the second half of the beam. In order to identify critical velocities of the full beam and amplification of additional displacement, other four curves are included. They correspond to maximum displacement directed downward and upward of an infinite beam of soft foundation and of strong foundation separately. Analogous results are presented in Figs. 15–17, but now for passage from the strong to the soft region.

From the figures it can be concluded, that there are two factors adversely affecting the response: first, the stronger region exhibit both critical velocities, which implies that for instance in the case with ratio 2 the strong region of critical velocity 235.0 m/s also gained critical velocity of 197.6 m/s. Also, it should be pointed out that in passage from softer to stronger region with factors 2 and 4, high displacements in both regions are obtained when the load is already in the second part of the structure. Second, it is clearly seen that maximum displacements are highly amplified as compared to the homogeneous situation, which, in the upward direction, has negative influence on vehicle stability and, in the downward direction augments foundation soils settlement and may induce track irregularities.

On the other hand analytical peaks from steady-state solution are smoothed in all cases. Generally, passage from stronger to softer region is less harmful, as expected.

6. Conclusions

Analytical transient solutions of dynamic response of one-dimensional systems with sudden change of foundation stiffness were analyzed and used for determination of critical velocities.

Two methodologies are proposed. One is based on the superposition of global modes of vibration, the other one is based on linking together analytical solutions of two separate parts of the structure. The results are expressed in terms of vertical displacement. There are no limitations on load velocity and presence of damping in both methodologies.

Although related to one-dimensional case, this study provides a first insight into the problem of excessive ground vibrations induced by high-speed trains in regions with vertical stiffness abrupt change. The transition radiation vibrations can be clearly visualized in the full range of velocities. The results obtained are used to study the influence of this abrupt change on critical velocities. This analysis is performed in a parametric way. It is shown that in the passage from softer to harder region, both critical velocities are clearly marked in the harder region. Moreover, the amplitudes of the maximum displacements are highly amplified. In the passage from harder to softer region this effect is not so evident.

Results and conclusions have direct application on estimates of ground vibrations induced by high-speed trains, and permit to evaluate the level of the additional loading factor to which high-speed trains and tracks must be designed. In these preliminary tests only a moving constant force is considered, and therefore the structure response is not always in accordance with what is experienced in high-speed railway practice. However, the interaction of the spring–mass–damper system of the vehicle with the rail and consequently with the track structure cannot be omitted. This subject is considered for further developments.

Acknowledgements

Results and conclusions presented here are partly included in the research project "Response of system railway track-soil to loads imposed by high-speed trains" POCI/ECM/61114/2004, funded by Fundação para a Ciência e a Tecnologia, from the Portuguese Ministry of Science and Technology.

References

[1] Lundqvist A, Dahlberg T. Railway track stiffness variations – consequences and countermeasures. In: Proceedings of the 19th IAVSD symposium on dynamics of vehicles on roads and on tracks, Milan, Italy; 2005.

[2] Metrikine AV, Wolfert ARM, Dieterman HA. Transition radiation in an elastically supported string. Abrupt and smooth variations of the support stiffness. Wave Motion 1998;27:291–305.

[3] Van Dalen KN. Ground vibration induced by a high-speed train running over inhomogeneous subsoil, transition radiation in two-dimensional inhomogeneous elastic systems. Master thesis, Department of Structural Engineering, TUDelft; 2006.
[4] Verichev SN, Metrikine AV. Instability of vibrations of a mass that moves uniformly along a beam on a periodically inhomogeneous foundation. J Sound Vib 2003;260:901–25.
[5] Ribeiro AC, Calçada R, Delgado R. Track–train dynamic behaviour on transition zones of high speed railway lines. In: Topping BHV, editor. Proceedings of the 11th international conference on civil, structural and environmental engineering computing. St. Julians, Malta: Civil-Comp Press; 2007.
[6] Andersen L, Nielsen SRK. Vibrations of a track caused by variations of the foundation stiffness. Probabilist Eng Mech 2003;18:171–84.
[7] Fröling RD. Low frequency dynamic vehicle/track interaction: modelling and simulation. Vehicle Syst Dyn 1998;28(Supplement):30–46.
[8] Release R2007a documentation for MATLAB. The MathWorks Inc.; 2007.
[9] Release 9 documentation for Maple.
[10] Release 11.0 documentation for ANSYS. Swanson Analysis Systems IP Inc.; 2007.
[11] Cottrell JA, Reali A, Bazilevs Y, Hughes TJR. Isogeometric analysis of structural vibrations. Comput Methods Appl Mech Eng 2006;195:5257–96.
[12] Frýba L. Vibration of solids and structures under moving loads. 3rd ed. London: Thomas Telford; 1999.
[13] Koloušek V. Dynamics of civil engineering structures. Part I – general problems. 2nd ed. Prague: SNTL; 1967 (in Czech).
[14] Chen Y-H, Sheu J-T. Beam length and dynamic stiffness. Comput Methods Appl Mech Eng 1996;129:311–8.